Splitting in the pinning-depinning transition of fronts in long-delayed bistable systems

Francesco Marino,[1] Giovanni Giacomelli,[2] and Stephane Barland[3]
[1]*CNR-Istituto Nazionale di Ottica, largo E. Fermi 6, I-50125 Firenze, Italy*
[2]*CNR-Istituto dei Sistemi Complessi, via Madonna del Piano 10, I-50019 Sesto Fiorentino, Italy*
[3]*Université Côte d'Azur, CNRS, INPHYNI, France*
(Received 11 January 2017; published 4 May 2017)

We investigate the formation of localized domains through front pinning in a periodically forced, bistable semiconductor laser with long-delayed optoelectronic feedback. At difference with 1D spatially extended systems, the transition from the pinning to the propagation regime occurs via two separated bifurcations, each corresponding to the unpinning of one of the fronts surrounding the localized domain. The bifurcation splitting is systematically explored, unveiling the crucial role played by the forcing frequency. The experimental results are reproduced and interpreted by means of a prototypical model of our system.

DOI: 10.1103/PhysRevE.95.052204

I. INTRODUCTION

The dynamics of fronts in spatially extended systems out of thermal equilibrium is of crucial importance in many areas of research, from chemical morphogenesis [1] to localized states in biological and optical systems [2].

In variational and spatially unidimensional bistable systems, it is well known that fronts connecting both phases will tend to drift at a velocity that is proportional to the asymmetry between the two phases, leading to stationary fronts only when both states have the same energy, i.e., at the so-called Maxwell point [3,4]. Therefore, starting from an inhomogeneous initial condition, in most cases the energetically favored phase will end up invading the whole system.

Following the first empirical [5,6] and later theoretical [7–9] works, showing a strong equivalence (for a review, see Ref. [10]) between spatially extended and delayed dynamical systems close to a supercritical Hopf bifurcation, it was recently shown experimentally [11,12] that bistable systems with delay can display a front dynamics, leading to a homogeneous state after a transient phase.

In spatially extended systems, several mechanisms can prevent the collapse of the fronts. In all cases, that leads to the formation of stable localized states consisting in islands of metastable phase surrounded by a sea of stable phase [13]. In optics, often invoked mechanisms are fronts pinning either to each other [14–16] or to some spatial modulation. This spatial modulation can either be intrinsic when one of the states is nonuniform [17,18] or extrinsic [19–21]. In the latter case, an external modulation is applied to a parameter, which breaks the translation invariance of an otherwise homogeneous state. In either case, the motion of fronts is strongly impacted, eventually reaching a pinning transition when the fronts do not move anymore, leading to the formation of localized domains.

In the delayed feedback experiment in Ref. [11], the interaction between neighboring fronts was attractive and therefore analogs of localized states could not be observed. Pursuing the idea of delimiting the boundaries of the analogy between delayed and spatially extended systems in the context of localized states (also explored in Refs. [22,23]), an experiment aiming at showing the front pinning transition has been recently performed [24] in a bistable laser system with optoelectronic feedback. In that case, the application of periodic forcing (analog of the spatial modulation) leads to the formation of localized states through front pinning, in a remarkably similar way to spatially extended systems. However, important features of these dynamics in delayed systems were not exhaustively analyzed. In particular, the unpinning transition appeared to be split in two distinct bifurcations, each corresponding to the unpinning of one of the fronts surrounding the localized domain. In the following, we explore systematically the bifurcation splitting, unveiling the role played by the parameters of the (pseudo-)spatial modulation.

II. EXPERIMENT

A. Experimental setup

The experimental setup is similar to that of Ref. [24] and it is shown in Fig. 1. A vertical cavity surface emitting laser (VCSEL) is operated in a regime of polarization bistability. One of the linear polarizations of the VCSEL is selected by a polarizing beam splitter and its intensity is monitored by a photodetector. The photodetector signal is then acquired and delayed (time delay $\tau = 19$ ms) by a digital reconfigurable acquisition board and subsequently fed back into the VCSEL through the pump current. The laser is biased by a dc voltage signal V_0 to which a periodic modulation $V_m \sin(2\pi t/T)$ provided by a function generator can be superimposed. The amplitude of the modulation is always kept much smaller than the width of the bistability region. The mutual stability of the two polarization states or, similarly, the tilt of the bistable potential, is controlled by V_0, which we will refer to as the asymmetry parameter. Here we use $V_0 = -453.3$ mV, for which the energetically favored phase is that corresponding to the high-intensity state. In order to observe the fronts and their motion in the pseudospace defined by the delayed feedback loop, a space-time representation [5] is created by decomposing the time series into pseudospatial cells of length $\tau + \varepsilon$, with $\varepsilon > 0$ due to causality [10]. Each time value within the time trace is identified by a real number σ ($0 \leqslant \sigma < \tau + \varepsilon$), indicating the position inside a given delay segment (the pseudospace) and by the segment number n, which plays the role of a discrete time.

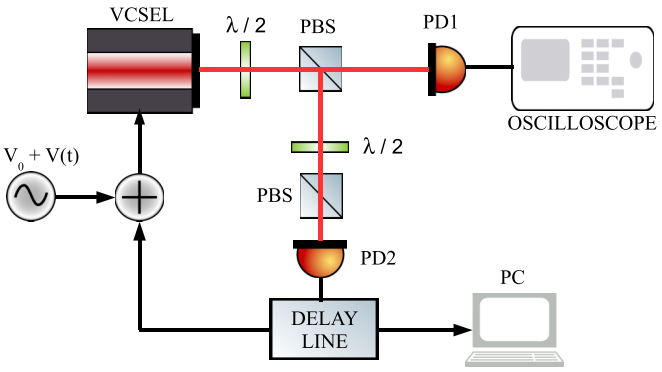

FIG. 1. Experimental setup. VCSEL, vertical cavity laser; $\lambda/2$, halfwave plate(s); PBS, polarizing beamsplitter(s); PD, photodetector(s). The modulation signal $V(t)$ is summed to the laser pump bias V_0. The delay line is realized with an A/D-D/A board suitably programed in a real-time Linux environment.

B. Experimental results

When the system is prepared in an inhomogeneous state, where the whole feedback loop is filled with the low power state with the exception of a small segment in the high-power state, coarsening is observed. The fronts propagate at constant speed without changing their shape, such that a single phase (the dominant) progressively invades the whole system. These dynamics are usually observed in 1D bistable media. However, along with their relative motion, fronts in long-delayed systems also exhibit a common drift. The average position of a phase domain is shifted to the right at each subsequent delay interval by a quantity $\delta \ll \tau$: the parity symmetry in pseudospace can be recovered in the tilted reference frame [11], i.e., by choosing $\varepsilon = \delta$ in the space-time representation. An example of these dynamics can be observed in Fig. 2, where we plot the evolution of the fronts speed and the corresponding spatiotemporal reconstruction. The velocity is calculated by detecting on the time series all occurrences of the rising or falling fronts and computing the temporal separation between consecutive occurrences. The difference between this temporal separation and the (known) delay time is the velocity $v_{\text{rise,fall}}$ of the front in a spatiotemporal representation. The constant δ is obtained in our case by $\delta = (v_{\text{rise}} + v_{\text{fall}})/2 - \tau = 5.11$ in units of sampling time and $\delta/\tau = 2.7 \times 10^{-3}$. In this reference frame, rising and falling fronts propagate symmetrically in the absence of pinning mechanism [up to 130 round trips in Figs. 2(a) and 2(b) and up to 90 round trips in Figs. 2(c) and 2(d)] and positive (negative) velocities correspond to fronts propagating to the right (left) direction.

When the modulation is switched on, the relative motion of the fronts is initially altered by the forcing and, after a short transient, is blocked (see Fig. 2). The front pinning is observed for small values of the asymmetry parameter, i.e., close to the Maxwell point, and the size of the pinning region depends on the strength of the spatial forcing.

While the modulation amplitude plays a very similar role with respect to the observations made, here the forcing frequency substantially changes the features of the pinning regime. In particular, for an arbitrary choice of T the average position of the high-intensity domain changes in the

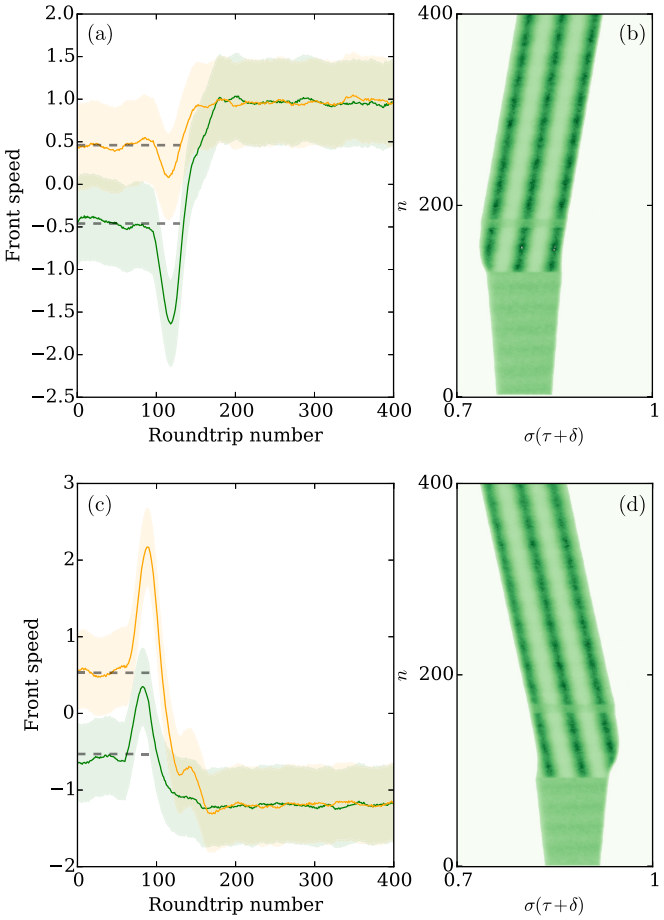

FIG. 2. Experiment. Spatiotemporal dynamics of fronts generated from a rectangular initial condition for different detunings. (a) Time evolution of the fronts speed and (b) the corresponding spatiotemporal plots: at time $n \sim 130$, the modulation is switched on, detuning $\gamma \approx -3 \times 10^{-4}$. (c) Time evolution of the fronts speed and (b) the corresponding spatiotemporal plots: at time $n \sim 90$, the modulation is switched on, detuning $\gamma \approx 2.5 \times 10^{-4}$. Asymmetry parameter $V_0 = -453.3$ mV, modulation amplitude $V_m = 1$ mV. On panels (a) and (c), the solid lines show the front velocity averaged (with Gaussian weights) over 30 roundtrips and the width of the stripes indicates the standard deviation of the velocity. This deviation is due to finite sampling rate of the measurement apparatus.

pseudotime. This is due to the fact that the periodic stable states of the system are stationary in the pseudotime only if the modulation period corresponds to an integer submultiple N_p of $(\tau + \delta)$. Otherwise, they exhibit a drift with a direction (velocity) determined by the sign (modulus) of the detuning parameter,

$$\gamma = (\tau + \delta)/T - N_p. \tag{1}$$

This is shown in Figs. 2(a), 2(c) and Figs. 2(b), 2(d) for negative and positive values of the detuning, respectively. For moderate values of γ the fronts are still pinned (their relative motion is frozen), but they are dragged by the underlying moving pattern.

A nonzero detuning affects also the pinning-depinning transition. In spatially extended bistable systems, the presence of the spatial forcing is known to induce an energy barrier

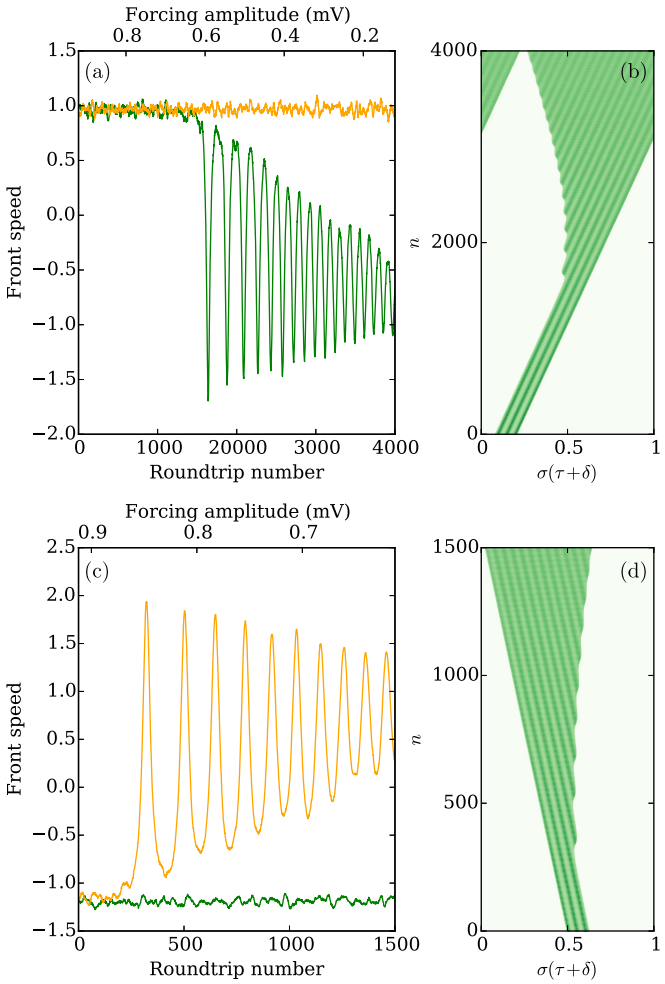

FIG. 3. Experiment. Spatiotemporal dynamics of fronts as the modulation amplitude is linearly decreased in time. (a) Time evolution of the fronts speed and (b) the corresponding spatiotemporal plots for $\gamma \approx -3 \times 10^{-4}$. (c) Time evolution of the fronts speed and (d) the corresponding spatiotemporal plots for $\gamma \approx 2.5 \times 10^{-4}$. Asymmetry parameter $V_0 = -453.3$ mV.

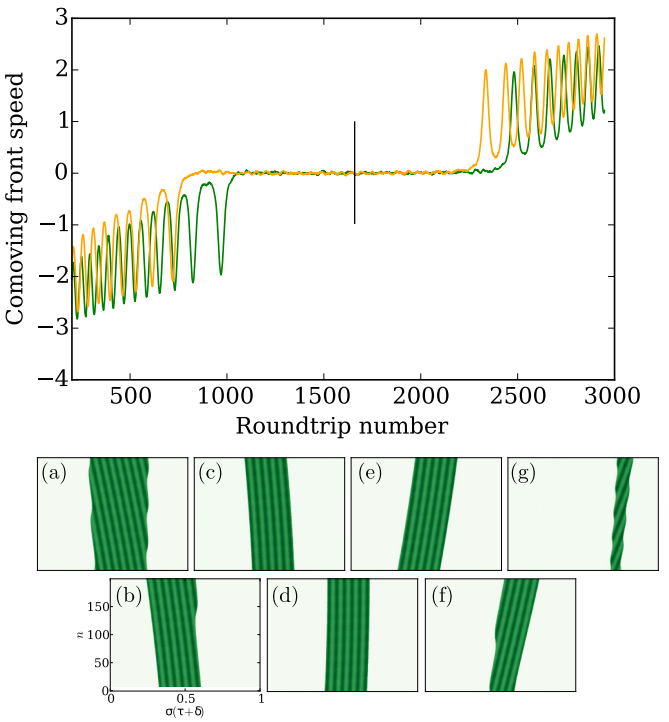

FIG. 4. Experiment. Spatiotemporal dynamics of fronts as the modulation frequency is varied. Main panel: time evolution of the comoving fronts velocities (see text). The vertical solid line indicates the point of effective zero detuning. Insets: spatiotemporal plots corresponding to different modulation frequencies (i.e., detunings) during the scan. Asymmetry parameter $V_0 = -453.3$ mV, modulation amplitude $V_m = 1$ mV.

for the front propagation to occur. Fixing the modulation amplitude and increasing the asymmetry parameter, a regime is found where the fronts start propagating with a velocity oscillating around a nonzero mean value. The same behavior is expected, keeping fixed the asymmetry and decreasing the modulation amplitude: the depinning of left and right fronts occurs for the same system parameters via a saddle node (on a circle-) bifurcation for the front velocities. On the contrary, here the transition from the pinning to the propagation regime occurs via two separated bifurcations.

In Fig. 3, we report the front velocities and the space time plots, for detunings as in Fig. 2, and keeping fixed the asymmetry. The modulation amplitude is slowly decreased, starting from values where both fronts are pinned. When the amplitude becomes sufficiently low, a first depinning transition is observed. The sign of the detuning determines which of the two fronts starts to propagate first, while its modulus determines the splitting between the bifurcations. For positive detunings, only the left front is propagating, whereas the right front is still pinned [see Figs. 3(a) and 3(b)]. Notice that the velocity of the left front is oscillating around a (negative) mean value with a frequency that increases with the distance to the bifurcation point. Since the modulation amplitude is continuously swept, it is not possible to extract the exact frequency scaling as a function of the bifurcation parameters (the frequency is barely constant over one period). However, the observed behavior as the depinning point is approached suggests the occurrence of an infinite-period bifurcation for the front velocities. For negative values of the detuning the opposite situations takes place: the right front is propagating while the left front remains pinned.

A more complete picture can be obtained by analyzing the system dynamics as a function of the detuning. As discussed above, changes of the forcing frequency correspond to variations of the detuning parameter. We thus analyze the spatiotemporal dynamics of fronts when the the modulation frequency is slowly varied, keeping fixed both the asymmetry and the modulation amplitude. Results are reported in Fig. 4. In the tilted reference frame $\tau + \delta$, in which free fronts propagate symmetrically, fronts locked to the forcing drift at a velocity proportional to the detuning γ. Here we plot the comoving fronts speed, defined as the front velocities with respect to the pseudospatial modulation. In this new reference frame, the fronts have zero velocity in the whole pinning region.

For modulation frequencies outside the locking range, both fronts are propagating with oscillating velocities. The number

of the velocity oscillations indicate the distance from the corresponding pinning bifurcation point. We remark, however, that also in this case, we are continuously scanning the bifurcation parameter and thus we cannot reconstruct the bifurcation diagram quantitatively. As shown in Fig. 4, inset (a), the velocity of the right front oscillates faster than that of the left front, indicating that the latter will undergo the pinning transition first. At a given point along the scan, we indeed observe that the left front is pinned while the right one is still propagating: this is a clear demonstration of the splitting in the pinning-depinning transition [see Fig. 4, inset (b)]. When the effective detuning is further decreased, the right front is pinned although both fronts are moving to the left [see Fig. 4, inset (c)]. A (nearly) stationary pattern in pseudotime is observed only very close to the point zero detuning [Fig. 4, inset (d)].[1] The same sequence of behavior is observed for positive detunings. However, the average position of the high-intensity phase is now moving to the right [Fig. 4, inset (e)] and is the left front the first to begin propagation [Fig. 4, inset (f)]. At higher values of the detuning, the second bifurcation takes place, as illustrated by the oscillating velocities in Fig. 4. This corresponds to the unpinning of the right front [Fig. 4, inset (g)].

III. NUMERICAL ANALYSIS

The polarization bistability in VCSELs can be described in terms of the competition of two polarization modes interacting with a single carrier density providing the optical gain. Under a suitable separation of the involved time scales, the VCSELs rate equations reduce to a one-dimensional double-well potential system, whose asymmetry parameter depends on the pump current [25,26]. Here, for the sake of simplicity and generality, we adopt a prototypical model with a cubic nonlinearity and a linear delayed feedback term [11]:

$$\dot{x} = -x(x+1+a)(x-1) + gx(t-\tau). \tag{2}$$

The time-dependent variable $x(t)$ describes how the total optical power is partitioned among the polarization modes and thus is related to the optical intensity in each polarization. The parameter a controls the degree of stability of the two stable states, $x_\pm = (-a \pm \sqrt{(2+a)^2+4g})/2$, and $g > 0$ is the feedback gain. As in the experiment, the system is prepared in an inhomogeneous initial condition $x_0(t) = x_- + x_+ \mathrm{rect}[(t-\tau/2)/w_0]$, $(-\tau \leqslant t < 0)$, corresponding to a rectangular-function profile of spatial width (w_0/τ), connecting the points $x_\pm$. The resulting spatiotemporal dynamics is visualized in the tilted reference frame, i.e., decomposing the time-series into pseudospatial cells of length $\tau + \delta$. As shown in Ref. [11], for $a \neq 0$ (asymmetric case), the system displays coarsening, i.e., propagating fronts separating two domains, each corresponding to one of the two stable states. When $a > 0$, the phase x_- gradually expands at the cost of the other one, leading eventually to a homogeneous state. For $a < 0$, the opposite situation takes place and from now on we shall restrict to this regime. The average growth rate of the dominant phase [dotted line in Fig. 5(a)] increases with $|a|$ and is zero only at the Maxwell point.

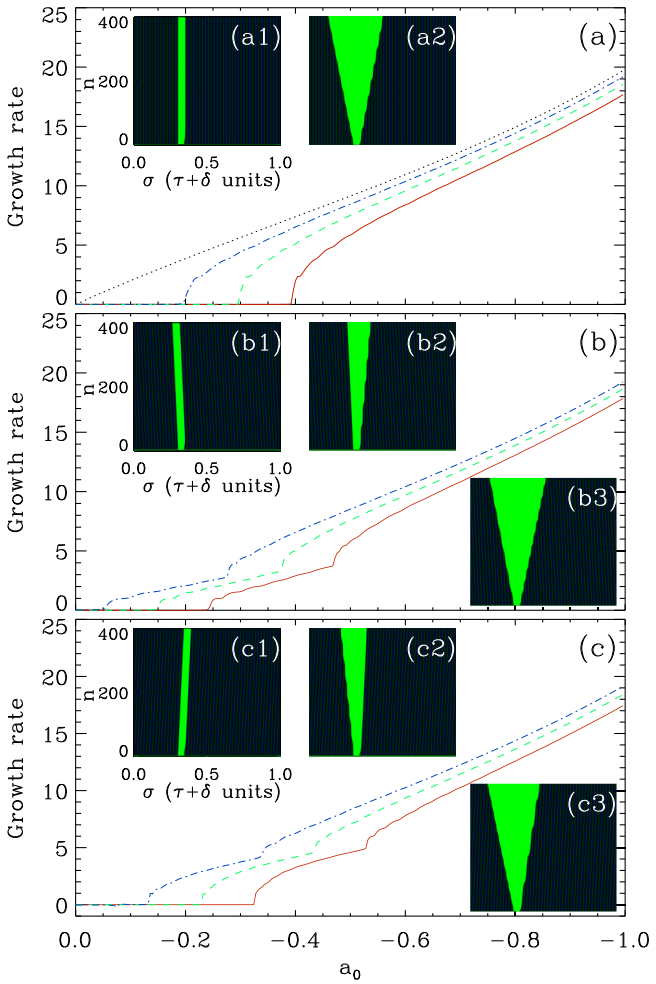

FIG. 5. Numerical results. Average growth rate of the dominant phase against the mean asymmetry parameter a_0, for different values of the detuning and of the modulation amplitude: (a) $\gamma = 0$; (b) $\gamma = 5 \times 10^{-3}$; (c) $\gamma = -5 \times 10^{-3}$. Dotted curves, $a_m = 0$; red (solid) curves $a_m = 0.4$; green (dashed) curves $a_m = 0.3$; blue (dot-dashed) curves $a_m = 0.2$. Insets: spatiotemporal plots of fronts corresponding to $a_m = 0.4$. $\gamma = 0$, $a_0 = -0.1$ (inset a1) and $a_0 = -0.6$ (inset a2). $\gamma = 5 \times 10^{-3}$, $a_0 = -0.1$ (inset b1), $a_0 = -0.4$ (inset b2) and $a_0 = -0.6$ (inset b3). $\gamma = -5 \times 10^{-3}$, $a_0 = -0.1$ (inset c1), $a_0 = -0.4$ (inset c2) and $a_0 = -0.6$ (inset c3). The system evolves starting from a rectangular-function profile $x_0(t)$ with $w_0 = 0.02\tau$ (see text). Other parameters: $g = 1$, $\tau = 100$, $N_p = 50$, $\delta \approx 1.35 \times 10^{-3}\tau$.

Pinning phenomena can be observed by applying a small temporal modulation to the asymmetry parameter,

$$a = a_0 + a_m \sin(2\pi t/T). \tag{3}$$

A crucial role is here played by the modulation period T that, for a given number of periods N_p in a pseudospatial cell $(\tau + \delta)$ uniquely determines the detuning parameter $\gamma = (\tau+\delta)/T - N_p$. When $a_m \neq 0$, the homogeneous states $x_\pm$ become periodic states in the pseudospace. We remind, however, that such states are stationary in the pseudotime only for zero detuning, i.e., when $T = (\tau+\delta)/N_p$, otherwise they exhibit a drift.

[1]The zero detuning point has been determined by fitting a straight line (corresponding to the linear scan of the forcing frequency) to the locked fronts displacements in the tilted reference frame, i.e., $\tau + \delta$.

We first consider the stationary case, $\gamma = 0$. In Fig. 5(a) we plot the average fronts velocity as a function of a_0, for three values of the modulation amplitude. For parameters next to the Maxwell point, we observe the existence of a pinning region where the average fronts velocity is zero. Within the pinning region, stationary stable localized states can be generated [see Fig. 5, inset (a1)] [24]. Outside this range, a regime is found where the fronts start propagating with a velocity oscillating around a nonzero mean value [see Fig. 5, inset (a2)]. In the tilted reference frame, the mean velocities of ascending (left) and descending (right) fronts have equal magnitude and opposite sign. When we increase the modulation amplitude, the pinning region grows, whereas the average front speed decreases. This behavior is reminiscent of what we observed in 1D spatially periodic media, where the transition from the pinning to the propagation regime occurs via a saddle-node bifurcation.

A substantially different behavior is observed when $\gamma \neq 0$ [see Figs. 5(b) and 5(c)]. In this case, the periodic modulation is no longer stationary in pseudotime. At low asymmetry parameters a pinning region still exists, where fronts have no relative motion and are pinned to the modulation pattern. As a consequence, the x_+ domain drifts while maintaining a constant width, thus defining a drifting localized structure [Fig. 5, insets (b1–c1)]. As $|a_0|$ increases, one of the fronts start propagating while the other remains pinned (see Fig. 5, insets (b2–c2)]. For larger values $|a_0|$, also the second front is eventually unpinned [Fig. 5, insets (b3–c3)]. Hence, for nonzero detunings the transition from the pinning to the propagation regime occurs via two separated saddle-node bifurcations. For $\gamma > 0$ the localized states propagate to the left and the right front is the first experiencing the bifurcation as $|a_0|$ increases [see Fig. 5(b)]. The opposite situation occurs for negative values of the detuning [see Fig. 5(c)].

The average growth rate of the x_+ phase, corresponding to two specific values of the asymmetry parameter, are displayed in Figs. 6(a)–6(c). For zero detuning, the growth rate decreases with the asymmetry parameter and abruptly drops to zero when $a_m = |a_0|$ [see Fig. 6(a)]. On the other hand, when $\gamma \neq 0$, the average growth rate generally experiences two separated transitions (see, e.g., dashed line in Figs. 6(b) and 6(c)], associated to the individual pinning of each front. For negative detunings and at very close to the Maxwell point, the intermediate region in which only one of the fronts is pinned is not observed. Instead, between the propagation and the pinning regime we observe a region where the growth rate is negative (fronts velocities have the same sign), leading to the consequent annihilation process. All these regimes can be clearly visualized in Figs. 6(d)–6(f), where we plot the phase diagrams of the system in the (a_m, a_0) plane for zero (d), positive (e), and negative (f) detunings. For $\gamma = 0$, the parameter space is separated into two parts. The fronts pinning (FP) region, whose size increases with the modulation amplitude, and the propagation region. The pinning regime exists even for arbitrarily small values of a_m, reducing to a single point (the Maxwell point) only at $a_m = 0$. In contrast for finite values of the detuning, at small modulation amplitudes the system displays just the propagation regime. In the propagation region PR1 (positive detunings), the right front propagates faster than the right one [see, e.g., inset (b3) of Fig. 5]. For negative detunings, the opposite situation takes place (propagation region PR2). As a_m is increased, a region appears in which one of the fronts is pinned while the other is propagating (left front pinned, LFP, when $\gamma > 0$ and right front pinned, RFP, when $\gamma < 0$). Here, for suitable values of a_0, the velocity of one of the fronts approximately matches the drift velocity of the modulation pattern, giving rise to a kind of locking phenomenon. Both LFP and RFP regions increase in size with a_m up to a certain maximum value. Beyond this point, they maintain a constant size, while appearing at growing values of the asymmetry parameter. At larger modulation amplitudes and for a_0 close to the Maxwell point, pinning phenomena are observed: the front pinning region FP1, in which localized states drifts to the left, and the region FP2, in which localized states drift to the right. Notice that, for $\gamma < 0$, we observe also a small region in which the average growth rate of the dominant phase x_+ decreases, leading eventually to the annihilation of fronts [annihilation region, AR, see also inset (c) in Fig. 6].

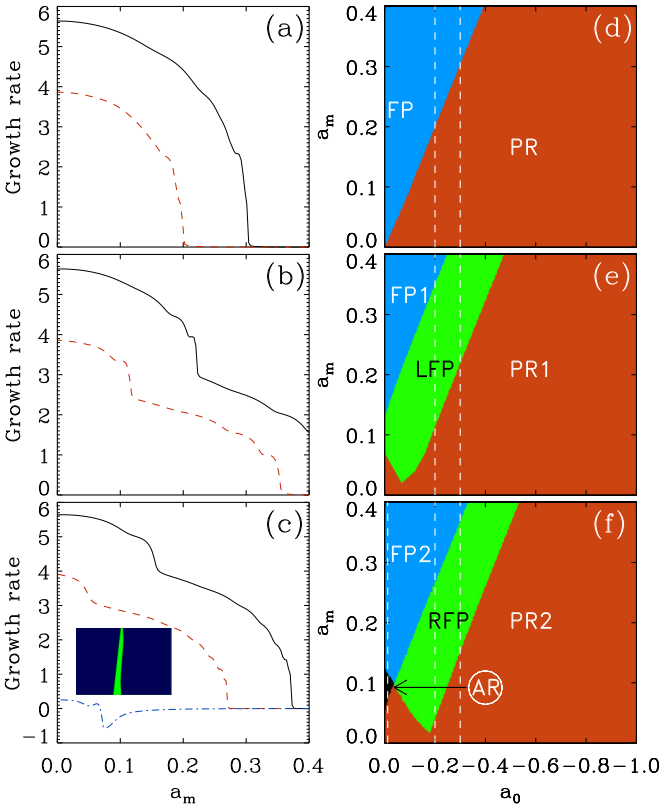

FIG. 6. Numerical results. Left panels: average growth rate of the dominant phase against the modulation amplitude, for different values of the detuning and of the mean asymmetry parameter. (a) $\gamma = 0$; (b) $\gamma = 5 \times 10^{-3}$; (c) $\gamma = -5 \times 10^{-3}$. Black (solid) curves, $a_0 = -0.3$; red (dashed) curves, $a_0 = -0.2$; blue (dot-dashed) curve $a_0 = -0.012$. The inset in panel (c) shows the spatiotemporal evolution of fronts corresponding to $a_0 = -0.012$ and $a_m = -0.08$. Right panels: phase diagram of the system in the (a_m, a_0) plane for (d) $\gamma = 0$; (e) $\gamma = 5 \times 10^{-3}$, (f) $\gamma = -5 \times 10^{-3}$ (see text). Other parameters as described in the caption of Fig. 5.

We finally complete our analysis by showing in Fig. 7 the phase diagram of the system in the (γ, a_0) plane for a

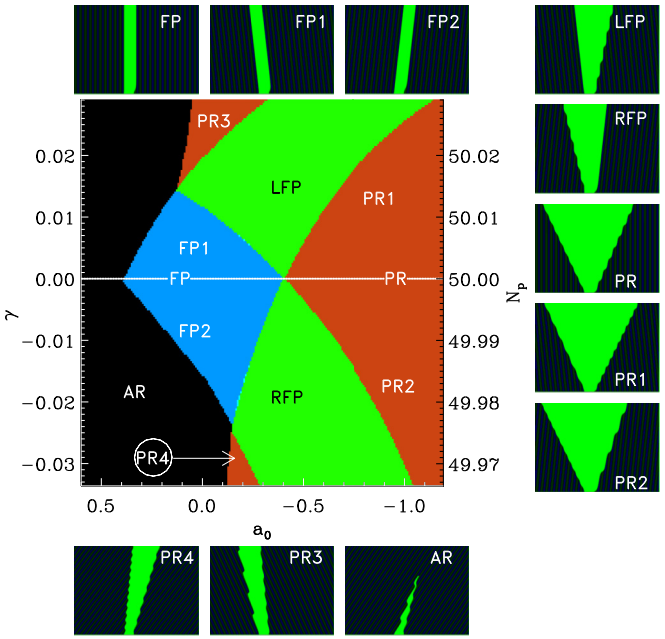

FIG. 7. Numerical results. Phase diagram of the system in the (γ, a_0) plane for $a_m = 0.4$ (see text) and examples of spatiotemporal plots in the different regions. Parameters corresponding to the spatiotemporal plots: (FP) $a_0 = -0.1$, $\gamma = 0$; (FP1) $a_0 = -0.1$, $\gamma = 5 \times 10^{-3}$; (FP2) $a_0 = -0.1$, $\gamma = -5 \times 10^{-3}$; (LFP) $a_0 = -0.4$, $\gamma = 5 \times 10^{-3}$; (RFP) $a_0 = -0.4$, $\gamma = -5 \times 10^{-3}$; (PR) $a_0 = -0.6$, $\gamma = -5 \times 10^{-3}$; (PR1) $a_0 = -0.6$, $\gamma = 5 \times 10^{-3}$; (PR2) $a_0 = -0.6$, $\gamma = -5 \times 10^{-3}$; (AR) $a_0 = -0.1$, $\gamma = 3 \times 10^{-2}$. Other parameters as described in the caption of Fig. 5.

fixed modulation amplitude. On the line $\gamma = 0$ the dynamics is reminiscent of what we observed in 1D bistable media with a spatially periodic modulation of the asymmetry parameter. Here, fixing the modulation amplitude, the size of the pinning region is maximal. At nonzero detunings, the system experiences an additional effective drift velocity. The main effect is to reduce the pinning region and to induce the appearance of the intermediate domains LFP and RFP, whose size gets wider as γ is increased. We point out that (i) the full diagram is not symmetric with respect to the transformation $\gamma \to -\gamma$ and (ii) $a_0 = 0$ does not necessarily show simultaneous unpinning. In spatially extended systems, both the average front velocity and the modulations are stationary, which corresponds to the case $\gamma = 0$, and the unpinning transition is not split, which appears to be a very particular case here.

IV. CONCLUSIONS

We have studied the dynamics of fronts in a periodically forced, bistable semiconductor laser with delayed optoelectronic feedback. In analogy to spatially extended media, we observe the formation of localized domains through front pinning, although the transitional regime exhibit some unique features, which are inherent to long-delayed systems. The unpinning transition appears to be split in two distinct bifurcations, each corresponding to the unpinning of one of the fronts surrounding the localized domain, a scenario that has not been described in spatially extended systems. Here this transition has been carefully studied, showing that for an arbitrary choice of the modulation period T, the stable states of the system are not stationary in pseudotime, leading to the formation of drifting localized states and to the aforementioned bifurcation splitting. Equivalently, the splitting of the unpinning transition is caused by the different front velocities with respect to the forcing when the latter is not stationary. The simultaneous unpinning of fronts is recovered in a very specific condition, when the modulation period corresponds to an integer submultiple of $(\tau + \delta)$, i.e., $\gamma = 0$, or when the modulation is stationary. Our experimental results, obtained in a bistable semiconductor laser with long-delayed feedback, are well described by a simplified prototypical model based on a one-dimensional double-well potential system with a cubic nonlinearity and a linear delayed feedback term. This clearly demonstrates that the phenomenology here described is independent of the physical details of the laser dynamics and thus is likely to be observed in any system with similar characteristics. In particular, we expect the pinning of fronts to (pseudo-)spatial modulation to present strong analogies with the pinning of localized states to temporal modulations both in delayed [27] and in propagative optical systems [28,29].

[1] A. M. Turing, Philos. Trans. R. Soc. London B **237**, 37 (1952).
[2] M. Tlidi, K. Staliunas, K. Panajotov, A. G. Vladimirov, and M. G. Clerc, Philos. Trans. R. Soc. London A **372**, 20140101 (2014).
[3] W. v. Saarloos, Phys. Rep. **386**, 29 (2003).
[4] Y. Pomeau, Physica D: Nonlinear Phenomena **23**, 3 (1986).
[5] F. T. Arecchi, G. Giacomelli, A. Lapucci, and R. Meucci, Phys. Rev. A **45**, R4225(R) (1992).
[6] G. Giacomelli, R. Meucci, A. Politi, and F. T. Arecchi, Phys. Rev. Lett. **73**, 1099 (1994).
[7] G. Giacomelli and A. Politi, Phys. Rev. Lett. **76**, 2686 (1996).
[8] M. Nizette, Physica D **183**, 220 (2003).
[9] M. Nizette, Phys. Rev. E **70**, 056204 (2004).
[10] S. Yanchuk and G. Giacomelli, J. Phys. A: Math. Theor. **50**, 103001 (2017).
[11] G. Giacomelli, F. Marino, M. A. Zaks, and S. Yanchuk, Europhys. Lett. **99**, 58005 (2012).
[12] J. Javaloyes, T. Ackemann, and A. Hurtado, Phys. Rev. Lett. **115**, 203901 (2015).
[13] P. Coullet, Int. J. Bifurcation Chaos Appl. Sci. Eng. **12**, 2445 (2002).
[14] N. Rosanov and S. Fedorov, Opt. Spectrosc. **72**, 782 (1992).
[15] N. N. Rosanov, *Spatial Hysteresis and Optical Patterns* (Springer-Verlag, Berlin/Heidelberg/New York, 2002).
[16] P. Parra-Rivas, E. Knobloch, D. Gomila, and L. Gelens, Phys. Rev. A **93**, 063839 (2016).
[17] S. Barbay, X. Hachair, T. Elsass, I. Sagnes, and R. Kuszelewicz, Phys. Rev. Lett. **101**, 253902 (2008).
[18] N. Verschueren, U. Bortolozzo, M. G. Clerc, and S. Residori, Phys. Rev. Lett. **110**, 104101 (2013).

[19] F. Haudin, R. G. Elías, R. G. Rojas, U. Bortolozzo, M. G. Clerc, and S. Residori, Phys. Rev. Lett. **103**, 128003 (2009).
[20] F. Haudin, R. G. Elías, R. G. Rojas, U. Bortolozzo, M. G. Clerc, and S. Residori, Phys. Rev. E **81**, 056203 (2010).
[21] F. Haudin, R. G. Rojas, U. Bortolozzo, S. Residori, and M. G. Clerc, Phys. Rev. Lett. **107**, 264101 (2011).
[22] B. Garbin, J. Javaloyes, G. Tissoni, and S. Barland, Nat. Commun. **6**, 5915 (2015).
[23] B. Romeira, R. Avó, J. M. Figueiredo, S. Barland, and J. Javaloyes, Sci. Rep. **6**, 19510 (2016).
[24] F. Marino, G. Giacomelli, and S. Barland, Phys. Rev. Lett. **112**, 103901 (2014).
[25] M. P. van Exter, A. Al-Remawi, and J. P. Woerdman, Phys. Rev. Lett. **80**, 4875 (1998).
[26] G. Giacomelli and F. Marin, Quant. Semiclass. Opt.: J. Eur. Opt. Soc. B **10**, 469 (1998).
[27] J. Javaloyes, P. Camelin, M. Marconi, and M. Giudici, Phys. Rev. Lett. **116**, 133901 (2016).
[28] J. K. Jang, M. Erkintalo, S. Coen, and S. G. Murdoch, Nat. Commun. **6**, 7370 (2015).
[29] J. K. Jang, M. Erkintalo, J. Schröder, B. J. Eggleton, S. G. Murdoch, and S. Coen, Opt. Lett. **41**, 4526 (2016).